CaMKII modulates sodium current in neurons from epileptic *Scn2a* mutant mice

Christopher H. Thompson[a,1], Nicole A. Hawkins[a], Jennifer A. Kearney[a], and Alfred L. George Jr.[a]

[a]Department of Pharmacology, Feinberg School of Medicine, Northwestern University, Chicago, IL 60611

Edited by Bruce P. Bean, Harvard Medical School, Boston, MA, and approved December 27, 2016 (received for review September 22, 2016)

Monogenic epilepsies with wide-ranging clinical severity have been associated with mutations in voltage-gated sodium channel genes. In the *Scn2a*^{Q54} mouse model of epilepsy, a focal epilepsy phenotype is caused by transgenic expression of an engineered $Na_V1.2$ mutation displaying enhanced persistent sodium current. Seizure frequency and other phenotypic features in *Scn2a*^{Q54} mice depend on genetic background. We investigated the neurophysiological and molecular correlates of strain-dependent epilepsy severity in this model. *Scn2a*^{Q54} mice on the C57BL/6J background (B6.Q54) exhibit a mild disorder, whereas animals intercrossed with SJL/J mice (F1.Q54) have a severe phenotype. Whole-cell recording revealed that hippocampal pyramidal neurons from B6.Q54 and F1.Q54 animals exhibit spontaneous action potentials, but F1.Q54 neurons exhibited higher firing frequency and greater evoked activity compared with B6.Q54 neurons. These findings correlated with larger persistent sodium current and depolarized inactivation in neurons from F1.Q54 animals. Because calcium/calmodulin protein kinase II (CaMKII) is known to modify persistent current and channel inactivation in the heart, we investigated CaMKII as a plausible modulator of neuronal sodium channels. CaMKII activity in hippocampal protein lysates exhibited a strain-dependence in *Scn2a*^{Q54} mice with higher activity in F1.Q54 animals. Heterologously expressed $Na_V1.2$ channels exposed to activated CaMKII had enhanced persistent current and depolarized channel inactivation resembling the properties of F1.Q54 neuronal sodium channels. By contrast, inhibition of CaMKII attenuated persistent current, evoked a hyperpolarized channel inactivation, and suppressed neuronal excitability. We conclude that CaMKII-mediated modulation of neuronal sodium current impacts neuronal excitability in *Scn2a*^{Q54} mice and may represent a therapeutic target for the treatment of epilepsy.

epilepsy | voltage-gated sodium channel | CaMKII

Voltage-gated sodium channels are essential for the generation and propagation of action potentials in excitable cells (1). These proteins exist as heteromultimeric complexes formed by a large pore-forming α-subunit and one or more auxiliary β-subunits (2). Function of voltage-gated sodium channels is influenced by multiple intracellular factors including protein–protein interactions, channel phosphorylation, and intracellular calcium. The auxiliary β-subunits and a family of FGF homologous factors (FHF) have been shown to modulate trafficking and functional properties of voltage-gated sodium channels (3–5). Both PKA and PKC have been shown to modulate neuronal voltage-gated sodium current function (6, 7). Finally, intracellular calcium, calmodulin, and calcium/calmodulin protein kinase II (CaMKII) have been shown to have drastic effects on the cardiac sodium channel (8–10). Thus, differences in posttranslational modification of sodium channels may profoundly influence the physiology of excitable cells.

Mutations in genes encoding neuronal voltage-gated sodium channels (*SCN1A*, $Na_V1.1$, and *SCN2A*, $Na_V1.2$) have been associated with several types of human epilepsy, including genetic epilepsy with febrile seizures plus ($GEFS^+$) and benign familial neonatal infantile seizures (BFNIS), and the more severe Dravet syndrome and early infantile epileptic encephalopathy type 11 (EIEE11) (2, 11). To date, more than 1,200 *SCN1A* mutations have been identified, making this gene the most frequently identified cause of monogenic epilepsy. Interestingly, variable expressivity is a common feature of monogenic epilepsy disorders, suggesting that genetic modifiers may contribute to clinical severity (12).

In *Scn2a*^{Q54} mice, transgenic expression of a gain-of-function sodium channel mutation results in epilepsy (13). Hippocampal pyramidal neurons isolated acutely from *Scn2a*^{Q54} mice exhibit enhanced persistent sodium current and spontaneous action potential firing. *Scn2a*^{Q54} mice congenic on the C57BL/6J strain (B6.Q54) show a progressive epilepsy beginning with spontaneous partial motor seizures that evolve to include secondary generalization as the mice age. *Scn2a*^{Q54} mice also exhibit a reduced life span compared with wild-type (WT) animals (13). Genetic background exerts a profound effect on phenotype severity in the *Scn2a*^{Q54} model. A single forward cross onto the SJL/J strain (F1.Q54) results in significant worsening of the epilepsy phenotype, with both increased seizure frequency and reduced life span compared with B6.Q54 animals (14).

Previous work identified two modifier loci that contribute to the strain difference in seizure frequency and severity in the *Scn2a*^{Q54} model (14). *Moe1* (modifier of epilepsy 1) involves multiple genes including *Cacna1g*, encoding the T-type Ca^{2+} channel $Ca_V3.1$, and *Hlf*, a PAR bZip transcription factor, whereas *Moe2* involves a single gene, *Kcnv2*, which encodes the silent K^+ channel subunit $K_V8.2$ (15-17). Additionally, RNA sequencing analysis of parent mouse strains revealed several other genes with divergent expression between mouse strains that may contribute to strain-dependent epilepsy severity, including genes directly involved in ion transport and posttranslational regulation of ion channel or transporters (18).

Significance

Epilepsy is a neurological disorder affecting approximately 1% of the world population. Mutations within genes encoding voltage-gated channels are the most frequently identified cause of monogenic epilepsies. Variable expressivity is a common feature of many epilepsies, suggesting that modifier genes make significant contributions to clinical phenotype. Here, we report an investigation of the molecular basis for strain-dependent seizure severity in the *Scn2a*^{Q54} epileptic mice. We show strain-dependent differences in pyramidal cell excitability correlate with divergent properties of voltage-gated sodium channels that could be explained by differences in calcium/calmodulin protein kinase II (CaMKII)-dependent modulation of neuronal sodium channels. These findings suggest that strain-dependent sodium channel modulation by CaMKII in *Scn2a*^{Q54} mice influences excitatory neuronal networks.

Author contributions: C.H.T., J.A.K., and A.L.G. designed research; C.H.T., N.A.H., and J.A.K. performed research; C.H.T., N.A.H., and J.A.K. analyzed data; and C.H.T., N.A.H., J.A.K., and A.L.G. wrote the paper.

The authors declare no conflict of interest.

This article is a PNAS Direct Submission.

[1]To whom correspondence should be addressed. Email: christopher.thompson1@northwestern.edu.

This article contains supporting information online at www.pnas.org/lookup/suppl/doi:10.1073/pnas.1615774114/-/DCSupplemental.

However, the underlying physiological mechanisms of strain-dependent epilepsy remain unexplored.

Here, we tested the hypothesis that strain-dependent seizure severity in *Scn2a*^{Q54} mice results from differential neuronal hyperexcitability stemming from divergent sodium channel properties between strains. We demonstrated that neurons from F1.Q54 animals exhibit enhanced excitability compared with B6.Q54 animals, have greater persistent sodium current, and have sodium channels that are more resistant to inactivation. Additionally, we discovered that CaMKII modulates neuronal voltage-gated sodium conductance and may be an important mediator of strain-dependent seizure severity. Thus, our findings indicate that the epilepsy phenotype of the *Scn2a*^{Q54} model may be, in part, driven by divergent strain-dependent sodium channel dysfunction and that CaMKII modulation of neuronal voltage-gated sodium current impacts neuronal excitability.

Results

Scn2a^{Q54} mice exhibit spontaneous focal epilepsy associated with enhanced persistent sodium current in acutely dissociated hippocampal neurons (13). Additionally, the phenotype shows a strong strain dependence, with animals on a congenic C57BL/6J background (B6.Q54) having a significantly less severe phenotype compared with animals intercrossed with WT SJL/J mice for a single generation (F1.Q54) (14). However, the neurophysiological basis for strain-dependent phenotype severity is unknown.

Strain-Dependent Neuronal Excitability. We hypothesized that differences in epilepsy severity observed between B6.Q54 and F1.Q54 animals correlate with differences in excitability of hippocampal pyramidal neurons. We used whole-cell current clamp recording to measure spontaneous and evoked action potential activity in pyramidal neurons isolated from transgenic animals of either background strain. Neurons isolated from WT animals exhibited minimal spontaneous action potential generation, as expected (Fig. 1 *A* and *B*). By contrast, and consistent with a spontaneous seizure phenotype, neurons from both strains of *Scn2a*^{Q54} animals fired spontaneous action potentials. However, neurons isolated from F1.Q54 animals exhibited a significantly higher frequency of spontaneous action potential firing compared with B6.Q54 animals (Fig. 1*C*; F1.Q54: 6.5 ± 1.5 Hz vs. B6.Q54: 2.5 ± 0.5 Hz, $n = 8–9$, $P < 0.05$).

In addition to spontaneous activity, we also measured evoked action potential firing. Similar to spontaneous activity, neurons isolated from F1.Q54 animals exhibited significantly greater evoked activity compared with neurons from B6.Q54 mice across a range of current injection amplitudes (Fig. 2). Neurons from F1.Q54 mice were more excitable at low amplitude current injections and showed sustained activity at stronger stimuli compared with neurons from B6.Q54 animals (Fig. 2 *A*–*C*). No differences between strains were detected in either input resistance (B6.Q54 = 1.9 ± 0.3 GΩ vs. F1.Q54 = 2.2 ± 0.4 GΩ) or action potential threshold (B6.Q54 = −42.7 ± 0.8 mV vs. F1.Q54 = −42.5 ± 0.8 mV). Additionally, neurons from F1.Q54 animals displayed a more narrow action potential width both at the beginning and end of a train of action potentials evoked by a 50-pA stimulus (Fig. 2*D*; first action potential: B6.Q54 = 3.1 ± 0.2 ms vs. F1.Q54 = 2.5 ± 0.1 ms, $P < 0.05$; final action potential: B6.Q54 = 5.1 ± 0.5 ms vs. F1.Q54 = 3.5 ± 0.4 ms, $P < 0.05$, $n = 8–9$). Interestingly, action potential duration increased significantly during a train of action potentials for B6.Q54 animals (first AP: 3.1 ± 0.2 ms vs. last AP: 5.1 ± 0.5 ms, $P < 0.05$), whereas that of F1.Q54 animals did not (first AP: 2.5 ± 0.1 ms vs. last AP: 3.5 ± 0.4 ms), suggesting an adaptive mechanism present in B6.Q54 animals is absent in neurons from F1.Q54 mice. These results indicate that the strain-dependent epilepsy severity observed for the *Scn2a*^{Q54} mouse model is correlated with divergent excitability of hippocampal pyramidal cells. Differences in action potential morphology between strains further suggest variable contribution of conductances necessary for action potential generation and propagation.

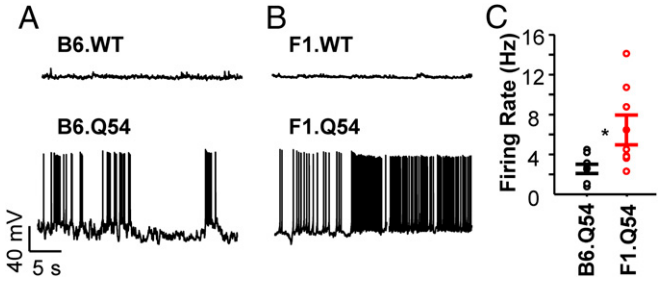

Fig. 1. Spontaneous action potential firing in pyramidal neurons. Representative current clamp recording of spontaneous action potentials from pyramidal neurons isolated from B6.WT and B6.Q54 (*A*) or F1.WT and F1.Q54 (*B*) mice. (*C*) Summary data for spontaneous action potential firing from B6.Q54 (black symbols) and F1.Q54 (red symbols) pyramidal neurons. Open symbols represent individual cells, whereas closed symbols are mean ± SEM for $n = 8–9$ measurements (*$P < 0.05$). There were no differences in spontaneous action potential firing frequency between nontransgenic mice on the two genetic backgrounds (B6.WT: 0.2 ± 0.2 Hz, vs. F1.WT: 0.3 ± 0.3 Hz; $n = 2$).

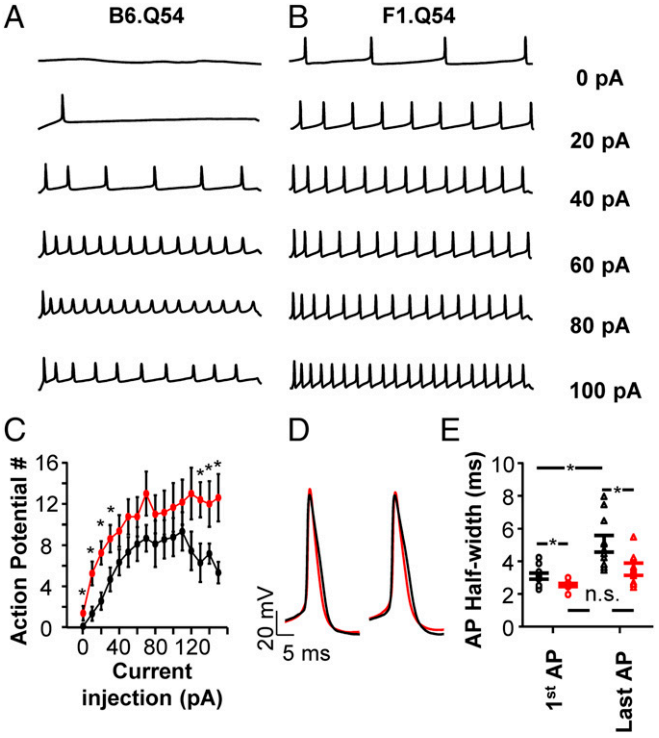

Fig. 2. Evoked action potentials in pyramidal neurons. Representative current clamp recordings of action potentials evoked by escalating amplitude of injected current from pyramidal neurons isolated from B6.Q54 (*A*) or F1.Q54 (*B*) mice. Cells were clamped to −80 mV and depolarizing current injections were made in 10-pA increments. (*C*) Summary data plotting the number of action potentials against current injection for B6.Q54 (black symbols) and F1.Q54 (red symbols) neurons. (*D*) Representative action potentials from either the second (*Left*) or final action potential (*Right*), evoked by a 50-pA current injection for either B6.Q54 (black trace) or F1.Q54 (red) trace. (*E*) Summary data of action potential half-width from either the first (circles) or final (triangles) action potential, evoked by a 50-pA current injection for either B6.Q54 (black) or F1.Q54 (red) neurons. Open symbols represent individual cells, whereas closed symbols are mean ± SEM for $n = 8–9$ cells (*$P < 0.05$; n.s., not significant).

NEUROSCIENCE

Strain-Dependent Biophysical Properties of Neuronal Sodium Conductance. The *Scn2a*^{Q54} model was originally generated with a specific defect in voltage-gated sodium channels that gives rise to enhanced persistent sodium current. To determine strain-dependent differences in sodium current, we performed whole-cell voltage clamp recordings from acutely dissociated hippocampal pyramidal neurons from B6.Q54 and F1.Q54 mice, as well as WT animals (B6.WT and F1.WT). Sodium currents from neurons isolated from B6.Q54 and F1.Q54 animals exhibited similar current–voltage relationships and peak current densities (Fig. 3 *A* and *B*, B6.Q54: −366.8 ± 55.2 pA/pF vs. F1.Q54: −308.5 ± 31.3 pA/pF, n = 12–15). Further, there were no differences in peak current densities between neurons isolated from the corresponding nontransgenic WT animals (Fig. S1*A*, B6.WT: −266.4 ± 37.9 pA/pF vs. F1.WT: −302.0 ± 32.5 pA/pF, n = 13–16). Comparison of voltage dependence of activation, and recovery from fast inactivation, between B6.Q54 and F1.Q54 animals showed no significant differences (Fig. 3 *C* and *D* and Table 1). However, neurons from F1.Q54 animals exhibited significantly depolarized steady-state channel availability compared with neurons from B6.Q54 animals (Fig. 3*C* and Table 1). This difference indicated that sodium channels present in F1.Q54 neurons are more resistant to inactivation compared with those present in B6.Q54 animals, and this phenomenon may contribute to neuronal hyperexcitability. Consistent with this hypothesis, neurons from F1.Q54 animals show a larger window current than B6.Q54 neurons, implying a broader voltage range over which F1.Q54 neurons remain active (Fig. S2). No differences in sodium channel properties were detected between WT strains (Fig. S1 and Table 1), which suggests that the observed difference in sodium channel inactivation is mediated by the transgene.

Strain Dependence of Persistent Sodium Current. We hypothesized that strain dependence of neuronal excitability may be due, in part, to differences in persistent sodium current between B6.Q54 and F1.Q54 animals. We found that B6.Q54 pyramidal neurons had persistent current levels that were not significantly different from WT mice (Table 1). However, pyramidal neurons isolated from F1.Q54 animals exhibited greater levels of persistent current compared with neurons from B6.Q54 mice (Fig. 3 *E* and *F*, 1.1 ± 0.2% vs. 0.4 ± 0.1, n = 6–8, $P < 0.05$). These data suggest that higher levels of persistent current in hippocampal pyramidal neurons correlate with enhanced excitability.

To exclude unequal transgene expression between B6.Q54 and F1.Q54 as an explanation for differences in persistent current, we quantified hippocampal transcript levels of rat $Na_V1.2$ by using quantitative digital droplet RT-PCR (ddRT-PCR). Using two separate assays that are specific for the transgene, we found no difference in hippocampal transgene levels between B6.Q54 and F1.Q54 animals (Fig. S3; Assay Rn00680558: B6.Q54, 0.19 ± 0.03 vs. F1.Q54, 0.22 ± 0.05; Assay Rn00561862: B6.Q54, 0.13 ± 0.02 vs. F1.Q54 0.15 ± 0.05), thereby excluding divergent expression of the transgene. Therefore, we considered other factors that could account for the differences in sodium channel behavior.

Strain-Dependent Hippocampal CaMKII Activity. Previous work has shown that the cardiac sodium channel $Na_V1.5$ can be modulated by intracellular Ca^{2+} and by CaMKII-mediated phosphorylation, which have profound effects on channel inactivation and persistent sodium current (8, 10, 19). Elevated intracellular Ca^{2+} has been demonstrated to evoke a depolarized shift in the voltage dependence of inactivation and suppression of persistent sodium current for cardiac $Na_V1.5$ channels (8, 20). Similarly, CaMKII-mediated phosphorylation of $Na_V1.5$ causes a shift in the voltage dependence of inactivation, as well as increased persistent sodium current (10, 19, 21, 22). We examined the effects of Ca^{2+} and CaMKII on the *Scn2a*^{Q54} mutant to determine whether these factors could explain the observed differences in channel inactivation and persistent sodium current.

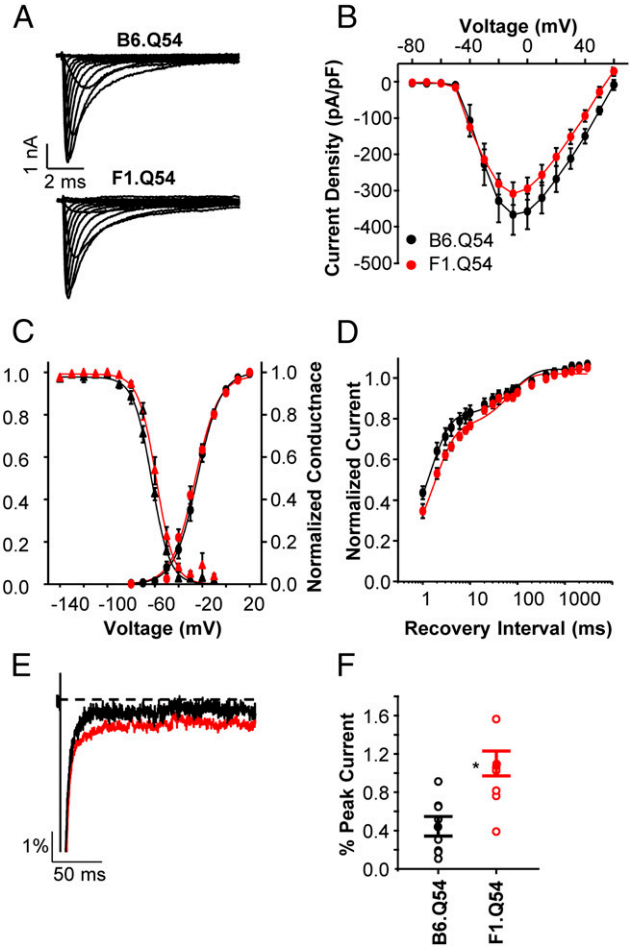

Fig. 3. Strain dependence of neuronal sodium current. (*A*) Representative whole-cell sodium current recordings from hippocampal pyramidal neurons isolated from either B6.Q54 (*Upper*) or F1.Q54 (*Lower*) mice. (*B*) Current–voltage relationship of voltage-dependent sodium channels from either B6.Q54 (black symbols) or F1.Q54 (red symbols) neurons. (*C*) Conductance voltage relationship (circles) and steady-state inactivation (triangles) of voltage-dependent sodium channels from either B6.Q54 (black symbols) or F1.Q54 (red symbols) neurons. (*D*) Recovery from inactivation of voltage-dependent sodium channels from either B6.Q54 (black symbols) or F1.Q54 (red symbols) neurons. (*E*) Representative normalized current trace illustrating persistent sodium current in response to a 200-ms depolarization (to 0 mV) from either B6.Q54 (black trace) or F1.Q54 (red trace) neurons. (*F*) Quantification of persistent current levels of B6.Q54 and F1.Q54 neurons expressed as percent of peak current. Open symbols represent individual cells, whereas closed symbols are mean ± SEM for n = 6–15 cells (*$P < 0.05$).

The voltage dependence of inactivation and magnitude of persistent sodium current were determined in the absence and presence of 1 μM free Ca^{2+} for heterologously expressed mutant rat $Na_V1.2$ channels ($Na_V1.2$-Q54; *SI Materials and Methods*), which is the *Scn2a*^{Q54} transgene. We observed no difference in the level of persistent sodium current between these two conditions (0 Ca^{2+}: 3.5 ± 0.4%; 1 μM Ca^{2+}: 3.1 ± 0.3%, n = 10–12, P = 0.48), and only a slight, but nonsignificant, depolarized shift in the voltage dependence of inactivation (0 Ca^{2+}: −65.1 ± 2.0 mV; 1 μM Ca^{2+}: −61.7 ± 1.8 mV, n = 10, P = 0.21; Fig. S4 *A–C*). These findings were consistent with previous reports showing no effect of intracellular Ca^{2+} on inactivation of WT $Na_V1.2$ channels (23). We conclude from these data that the strain differences in neuronal sodium current properties do not depend strictly on intracellular Ca^{2+} concentration.

Table 1. Biophysical properties of *Scn2a*^{Q54} neuronal sodium channels

	Voltage dependence of activation			Voltage dependence of fast inactivation			Recovery from fast inactivation			Persistent current	
Strain	$V_{1/2}$, mV	k, mV	n	$V_{1/2}$, mV	k, mV	n	τ_f, ms (amplitude)	τ_s, ms (amplitude)	n	% peak current	n
B6.WT	−23.4 ± 1.7	8.6 ± 0.6	13	−60.9 ± 1.9	−7.1 ± 0.2	7	1.2 ± 0.1 (0.68 ± 0.04)	65.4 ± 9.8 (0.33 ± 0.03)	7	0.5 ± 0.2	8
B6.Q54	−24.9 ± 1.9	9.0 ± 0.5	12	−63.2 ± 1.0	−7.9 ± 0.8	6	1.4 ± 0.1 (0.80 ± 0.04)	119.1 ± 24.5 (0.23 ± 0.04)	7	0.4 ± 0.1	8
F1.WT	−22.2 ± 1.8	9.9 ± 0.9	16	−62.2 ± 1.3	−7.4 ± 0.4	12	1.5 ± 0.1 (0.76 ± 0.02)	79.6 ± 7.9 (0.25 ± 0.01)	10	0.5 ± 0.2	5
F1.Q54	−26.5 ± 1.5*	9.0 ± 0.4	15	−59.6 ± 1.0†	−7.1 ± 0.4	10	1.9 ± 0.2 (0.73 ± 0.02)	81.8 ± 10.4 (0.28 ± 0.02)	11	1.1 ± 0.2†	6

*$P < 0.05$ compared with nontransgenic animals of the same genetic background.
†$P < 0.05$ compared with B6.Q54 animals.

To determine whether divergent CaMKII-mediated phosphorylation underlies strain-dependent differences in voltage-gated sodium current, we quantified basal and maximal CaMKII activity from hippocampal protein lysates from B6.Q54 and F1.Q54 animals, and WT littermates. Basal hippocampal CaMKII activity measured in samples from F1.Q54 animals was significantly greater than in samples from B6.Q54 animals (2.3 ± 0.16 A.U. vs. 1.8 ± 0.07 A.U., $P < 0.05$, $n = 5$; Fig. 4*A*). Levels of maximal CaMKII activity, which were measured after adding exogenous Ca^{2+} and CaM to protein lysates, were not different between *Scn2a*^{Q54} strains (B6.Q54, 2.8 ± 0.2 A.U.; F1.Q54, 2.6 ± 0.6 A.U., $P = 0.79$, $n = 5$; Fig. 4*B*). Further, basal CaMKII activity normalized to maximal activity was significantly greater in samples from F1.Q54 mice compared with B6.Q54 animals (88.4 ± 3.6% vs. 68.2 ± 4.8%, $P < 0.05$, $n = 5$; Fig. 4*C*). There were no differences in basal or maximal CaMKII activity between WT littermates from the different genetic backgrounds (B6.WT, basal, 1.8 ± 0.03 A.U., maximal, 2.6 ± 0.04 A.U., $n = 3$; F1.WT, basal, 1.8 ± 0.05 A.U., maximal, 2.6 ± 0.07 A.U., $n = 5$). These differences suggest that differential CaMKII activity between mouse strains may contribute to strain-dependent differences in seizure severity in *Scn2a*^{Q54} mice.

Regulation of Sodium Channel Inactivation by CaMKII. We assessed whether CaMKII modulates persistent sodium current and voltage dependence of channel inactivation exhibited by heterologously expressed $Na_V1.2$-Q54. When activated CaMKII monomer was included in the intracellular pipette solution, persistent sodium current mediated by $Na_V1.2$-Q54, was 8.5 ± 2.5% ($n = 6$) compared with 2.8 ± 0.4% for cells exposed to vehicle alone ($n = 6$, $P < 0.05$; Fig. 5*A*). Additionally, we observed a large depolarized shift in the voltage dependence of inactivation compared with cells exposed to vehicle (Fig. 5*A*, −49.6 ± 1.2 mV vs. −61.9 ± 2.4 mV, $n = 3$–5, $P < 0.05$). Importantly, we found that CaMKII exerts similar effects on WT $Na_V1.2$ to enhance persistent sodium current (CaMKII = 2.0 ± 0.4%; Vehicle = 0.5 ± 0.2%, $n = 6$, $P < 0.05$; Fig. 5*B*) and induce a large depolarized shift in the voltage dependence of inactivation (−43.7 ± 1.5 mV vs. −56.4 ± 1.1 mV, $n = 4$–5, $P < 0.05$; Fig. 5*B*).

We also compared persistent current and steady-state inactivation in pyramidal neurons isolated from F1.Q54 animals pretreated with either KN-93, a CaMKII inhibitor, or KN-92, an inactive analog. Fig. 5*C* illustrates that neurons treated with KN-93 exhibited virtually no persistent current (0.1 ± 0.1% $n = 6$) and a hyperpolarized $V_{1/2}$ for steady-state inactivation ($V_{1/2} = -73.9$ ± 2.2 mV, $n = 6$) compared with neurons treated with KN-92 (0.96 ± 0.2% $n = 7$, $V_{1/2} = -64.9 \pm 2.3$ mV, $n = 7$, $P < 0.05$, compared with KN-93–treated cells). Finally, we compared spontaneous firing frequency of neurons treated intracellularly with 1 μM KN-93 or 1 μM KN-92 and found that suppression of CaMKII activity with KN-93 abolished spontaneous firing of F1.Q54 neurons (0.06 ± 0.04 Hz, $n = 7$). By contrast, neurons treated with KN-92 exhibited a high spontaneous firing frequency (5.4 ± 1.1 Hz, $n = 7$, $P < 0.05$; Fig. 6 *A* and *B*) similar to untreated cells. We also observed that KN-93–treated neurons showed less evoked action potential firing compared with neurons treated with KN-92 (Fig. 6*C*). These data support our hypothesis that differential modulation of sodium channels by CaMKII significantly impacts neuronal excitability.

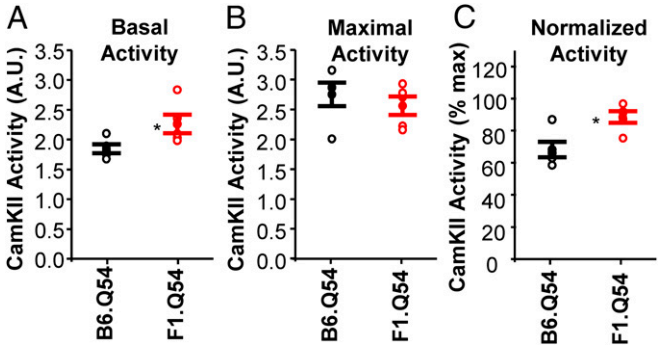

Fig. 4. Strain dependence of hippocampal CaMKII activity. (*A*) Basal CaMKII activity of hippocampal protein lysates from B6.Q54 (black symbols) or F1.Q54 (red symbols) reported as absorbance at 450 nM. (*B*) Maximal CaMKII activity following stimulation with Ca^{2+}/CaM measured in hippocampal protein lysates from B6.Q54 (black symbols) or F1.Q54 (red symbols) reported as absorbance at 450 nM. (*C*) Basal CaMKII activity normalized to maximal activity for B6.Q54 (black symbols) or F1.Q54 (red symbols). Open symbols represent individual animals, whereas closed symbols are mean ± SEM for $n = 5$ animals (*$P < 0.05$).

Discussion

Mutations in voltage-gated sodium channel genes are associated with a spectrum of genetic epilepsies that may exhibit variable expressivity, which is attributable in part to the action of genetic modifiers. The influence of genetic modifiers on variable expressivity can be studied by using engineered mice bearing mutations in sodium channel genes. In this study, we examined the strain-dependent seizure severity observed in the gain-of-function *Scn2a*^{Q54} epileptic mouse and identified neurophysiological features that may contribute to variable phenotype expression.

The *Scn2a*^{Q54} mouse model exhibits spontaneous seizures originating within the hippocampus, the severity of which depends greatly on genetic background. These mice show increased persistent sodium current as a result of mutant *Scn2a* transgene expression, and this phenomenon is a plausible contributing factor to epilepsy. Extracellular recording of hippocampal slices from F1.Q54 animals showed that both the CA1 and CA3 regions show spontaneous action potential firing not present in WT mice (24). Additionally, brain slices from F1.Q54 animals have greater spontaneous and after-discharge activity following tetanic stimulation (24). Consistent with this prior work, we demonstrated that hippocampal pyramidal neurons isolated from WT animals show no spontaneous action potentials, but pyramidal neurons isolated acutely from either B6.Q54 or F1.Q54 animals exhibit spontaneous action potentials, with cells from F1.Q54 mice having a higher

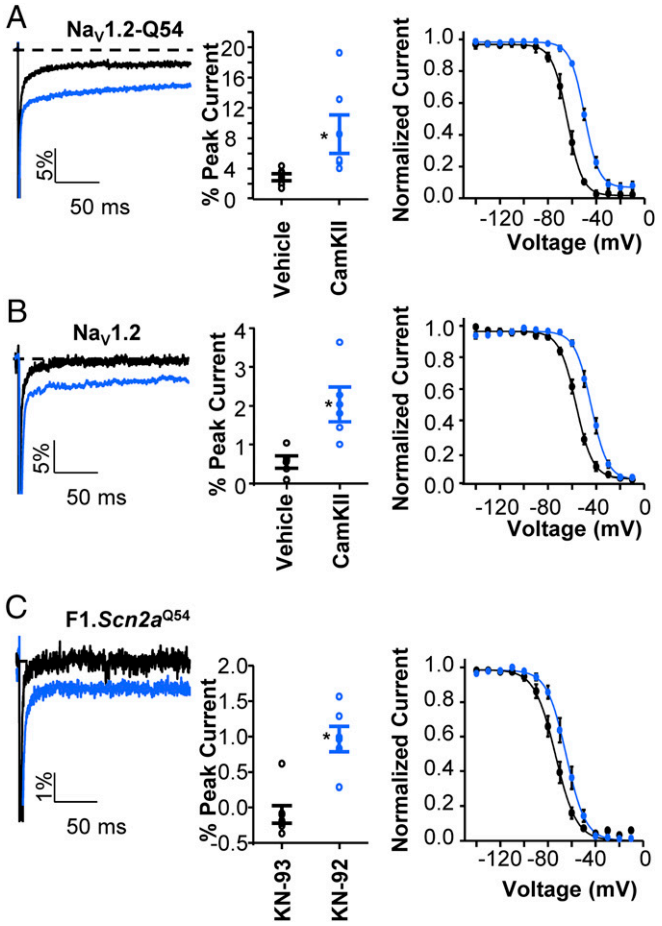

Fig. 5. CaMKII regulation of voltage-gated sodium current. (*A* and *B, Left*) Representative normalized current trace illustrating persistent sodium current in response to a 200-ms depolarization (to 0 mV) recorded from HEK293T cells transfected with Na$_V$1.2-Q54 (*A*) or Na$_V$1.2-WT (*B*) in the presence of activated CaMKII monomer (blue trace) or vehicle (black trace). (*A* and *B, Center*) Quantification of persistent current levels of Na$_V$1.2-Q54 (*A*) or Na$_V$1.2-WT (*B*) in the presence of activated CaMKII monomer or vehicle expressed as percent of peak current. (*A* and *B, Right*) Steady-state inactivation for sodium channels in the presence of activated CaMKII monomer (blue symbols) or vehicle (black symbols). (*C, Left*) Representative normalized current trace illustrating persistent sodium current in response to a 200-ms depolarization (to 0 mV) recorded from F1.Q54 pyramidal neurons in the presence of 10 μM KN-93 (black trace) or 10 μM KN-92 (blue trace). (*C, Center*) Quantification of persistent current levels from pyramidal neurons in the presence of 10 μM KN-93 or 10 μM KN-92 expressed as percent of peak current. (*C, Right*) Steady-state inactivation for sodium channels in the presence of 10 μM KN-93 (black symbols) or 10 μM KN-92 (blue symbols). Open symbols represent individual cells, whereas closed symbols are expressed as mean ± SEM for $n = 3$–7 cells (*$P < 0.05$).

firing frequency. Additionally, F1.Q54 animals exhibit significantly greater evoked action potential firing.

Action potential morphology is an important contributor to neuronal firing frequency, with high frequency firing being associated with narrow action potential width (25). We observed that pyramidal neurons from F1.Q54 mice exhibited narrower action potentials compared with neurons from B6.Q54 animals. Moreover, neurons from B6.Q54 animals exhibited a trend toward a greater degree of action potential broadening during a train of action potentials compared with neurons from F1.Q54 animals (Fig. 2), consistent with the hypothesis that excitatory neurons from F1.Q54 animals can maintain higher firing rates for longer periods of time and may promote a more severe seizure phenotype. Although increased persistent current is predicted to broaden action potentials in neurons from F1.Q54 mice, previously reported strain-dependent differences in K^+ channel expression may also contribute in a manner opposing the effect of enhanced sodium current (15). Specifically, B6.Q54 mice express a higher level of *Kcnv2*, a silent K^+ channel subunit that forms heterotetramers with K_V2.1 and suppresses delayed rectifier current. Reduced K_V2.1-mediated current is predicted to enhance excitability of neurons from B6.Q54 mice, similar to what has been demonstrated for K_V2.1 knockout mice, and evoked action potential broadening during a train of action potentials (26), which is what we observed in this study (Fig. 2).

We observed no strain differences in sodium channel properties measured from WT neurons. By contrast, neurons isolated from F1.Q54 animals exhibited higher levels of persistent current and a depolarized steady-state inactivation compared with B6.Q54 mice. A consequence of the shift in steady-state inactivation for F1.Q54 animals compared with B6.Q54 animals is a larger window current, which has been shown to be a common feature of cardiac arrhythmias resulting from mutations in *SCN5A* (27, 28). The greater tendency for spontaneous action potential firing observed in F1.Q54 neurons may be a result of both increased persistent current and increased window current. Importantly, the larger persistent sodium current could not be explained by differences in transgene expression within brain regions we used to isolate neurons for electrophysiological recording. These observations suggest the existence of other factors that may modulate sodium channels.

We sought to understand the basis for different persistent current levels between B6.Q54 and F1.Q54 animals. Phosphorylation of sodium channels is a critical regulator of channel activity, with phosphorylation state changing dramatically as a function of seizure activity in the brain (6, 7). In the heart, CaMKII phosphorylation has been shown to enhance persistent sodium current and induce a shift in steady-state channel availability (19). Although the sites for CaMKII phosphorylation of Na$_V$1.5 are not perfectly conserved across all sodium channels, 24 of 36 CaMKII phosphorylation sites identified by either mass spectrometry analysis or functional analyses, including the critical sites S516 and S571, are conserved in rodent Na$_V$1.2 (10, 21). Our experiments demonstrated that hippocampal lysates from *Scn2a*^{Q54} mouse strains have divergent levels of CaMKII activity. Previous reports have shown that CaMKII autophosphorylation is initially reduced in various epilepsy models, including

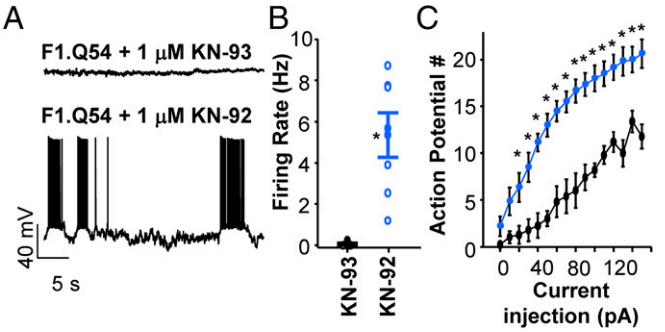

Fig. 6. CaMKII regulation of neuronal excitability. (*A*) Representative current clamp recordings of spontaneous action potential activity from F1.Q54 animals in the presence of either 1 μM intracellular KN-93 (*Upper*) or 1 μM KN-92 (*Lower*). (*B*) Summary data for spontaneous action potential firing from KN-93 (black symbols) and KN-92 (blue symbols) treated pyramidal neurons. Open symbols represent individual cells. (*C*) Summary data plotting the number of action potentials against current injection for KN-93 (black symbols) and KN-92 (blue symbols) treated neurons. Closed symbols represent mean ± SEM for $n = 5$–7 measurements (*$P < 0.05$).

pilocarpine and kainic acid-induced seizure models, but total CaMKII protein may be increased in prolonged timepoints following seizure onset (29–31). Interestingly, WT littermates do not show strain dependence of CaMKII activity, suggesting that seizures may also influence CaMKII activity in the hippocampus of *Scn2a*^{Q54} mice. Although our findings strongly support CaMKII modulation of neuronal sodium current and excitability of neurons from *Scn2a*^{Q54} mice, we cannot exclude epileptogenic effects of CaMKII on other cellular targets that also have strain dependence.

In summary, our work demonstrated CaMKII modulation of neuronal sodium channels in heterologous cells and in acutely isolated neurons from a mouse model of epilepsy. CaMKII evokes a mechanism to regulate neuronal sodium current in a manner that impacts neuronal excitability. Pharmacological strategies for suppressing CaMKII activity in brain might conceivably exert antiepileptic effects.

Materials and Methods

All experiments were approved by the Animal Care and Use Committee of Northwestern University in accordance with the National Institutes of Health *Guide for the Care and Use of Laboratory Animals* (32). Hippocampal neuron dissociations were performed as described (33). All mutagenesis, heterologous expression, voltage-clamp, and current-clamp recordings were performed as described (33–37). For description of materials and methods used, see *SI Materials and Methods*.

ACKNOWLEDGMENTS. We thank Sunita Misra for initial assistance with project and Jeffrey Calhoun, Alison Miller, Clint McCollom, and Nicole Zachwieja for mouse colony assistance. This work was supported by Epilepsy foundation Postdoctoral Fellowship 189645 (to C.H.T.) and NIH Grants NS053792 (to J.A.K.) and NS032387 (to A.L.G.).

1. Catterall WA, Kalume F, Oakley JC (2010) $Na_V1.1$ channels and epilepsy. *J Physiol* 588(Pt 11):1849–1859.
2. George AL, Jr (2005) Inherited disorders of voltage-gated sodium channels. *J Clin Invest* 115(8):1990–1999.
3. Wang C, Wang C, Hoch EG, Pitt GS (2011) Identification of novel interaction sites that determine specificity between fibroblast growth factor homologous factors and voltage-gated sodium channels. *J Biol Chem* 286(27):24253–24263.
4. Pablo JL, Wang C, Presby MM, Pitt GS (2016) Polarized localization of voltage-gated Na^+ channels is regulated by concerted FGF13 and FGF14 action. *Proc Natl Acad Sci USA* 113(19):E2665–E2674.
5. Yan H, Pablo JL, Wang C, Pitt GS (2014) FGF14 modulates resurgent sodium current in mouse cerebellar Purkinje neurons. *eLife* 3:e04193.
6. Baek JH, Rubinstein M, Scheuer T, Trimmer JS (2014) Reciprocal changes in phosphorylation and methylation of mammalian brain sodium channels in response to seizures. *J Biol Chem* 289(22):15363–15373.
7. Scheuer T (2011) Regulation of sodium channel activity by phosphorylation. *Semin Cell Dev Biol* 22(2):160–165.
8. Potet F, Beckermann TM, Kunic JD, George AL, Jr (2015) Intracellular calcium attenuates late current conducted by mutant human cardiac sodium channels. *Circ Arrhythm Electrophysiol* 8(4):933–941.
9. Van Petegem F, Lobo PA, Ahern CA (2012) Seeing the forest through the trees: Towards a unified view on physiological calcium regulation of voltage-gated sodium channels. *Biophys J* 103(11):2243–2251.
10. Ashpole NM, et al. (2012) Ca^{2+}/calmodulin-dependent protein kinase II (CaMKII) regulates cardiac sodium channel $Na_V1.5$ gating by multiple phosphorylation sites. *J Biol Chem* 287(24):19856–19869.
11. Meisler MH, Kearney JA (2005) Sodium channel mutations in epilepsy and other neurological disorders. *J Clin Invest* 115(8):2010–2017.
12. Meisler MH, O'Brien JE, Sharkey LM (2010) Sodium channel gene family: Epilepsy mutations, gene interactions and modifier effects. *J Physiol* 588(Pt 11):1841–1848.
13. Kearney JA, et al. (2001) A gain-of-function mutation in the sodium channel gene *Scn2a* results in seizures and behavioral abnormalities. *Neuroscience* 102(2):307–317.
14. Bergren SK, Chen S, Galecki A, Kearney JA (2005) Genetic modifiers affecting severity of epilepsy caused by mutation of sodium channel Scn2a. *Mamm Genome* 16(9):683–690.
15. Jorge BS, et al. (2011) Voltage-gated potassium channel *KCNV2* (Kv8.2) contributes to epilepsy susceptibility. *Proc Natl Acad Sci USA* 108(13):5443–5448.
16. Hawkins NA, Kearney JA (2016) *Hlf* is a genetic modifier of epilepsy caused by voltage-gated sodium channel mutations. *Epilepsy Res* 119:20–23.
17. Calhoun JD, Hawkins NA, Zachwieja NJ, Kearney JA (2016) Cacna1g is a genetic modifier of epilepsy caused by mutation of voltage-gated sodium channel Scn2a. *Epilepsia* 57(6):e103–e107.
18. Hawkins NA, Kearney JA (2012) Confirmation of an epilepsy modifier locus on mouse chromosome 11 and candidate gene analysis by RNA-Seq. *Genes Brain Behav* 11(4):452–460.
19. Aiba T, et al. (2010) Na^+ channel regulation by Ca^{2+}/calmodulin and Ca^{2+}/calmodulin-dependent protein kinase II in guinea-pig ventricular myocytes. *Cardiovasc Res* 85(3):454–463.
20. Wingo TL, et al. (2004) An EF-hand in the sodium channel couples intracellular calcium to cardiac excitability. *Nat Struct Mol Biol* 11(3):219–225.
21. Herren AW, et al. (2015) CaMKII phosphorylation of $Na_{(V)}1.5$: Novel in vitro sites identified by mass spectrometry and reduced S516 phosphorylation in human heart failure. *J Proteome Res* 14(5):2298–2311.
22. Hund TJ, et al. (2010) A β(IV)-spectrin/CaMKII signaling complex is essential for membrane excitability in mice. *J Clin Invest* 120(10):3508–3519.
23. Wang C, et al. (2014) Structural analyses of Ca^{2+}/CaM interaction with NaV channel C-termini reveal mechanisms of calcium-dependent regulation. *Nat Commun* 5:4896.
24. Kile KB, Tian N, Durand DM (2008) *Scn2a* sodium channel mutation results in hyperexcitability in the hippocampus in vitro. *Epilepsia* 49(3):488–499.
25. Bean BP (2007) The action potential in mammalian central neurons. *Nat Rev Neurosci* 8(6):451–465.
26. Speca DJ, et al. (2014) Deletion of the Kv2.1 delayed rectifier potassium channel leads to neuronal and behavioral hyperexcitability. *Genes Brain Behav* 13(4):394–408.
27. Beckermann TM, McLeod K, Murday V, Potet F, George AL, Jr (2014) Novel SCN5A mutation in amiodarone-responsive multifocal ventricular ectopy-associated cardiomyopathy. *Heart Rhythm* 11(8):1446–1453.
28. Nguyen TP, Wang DW, Rhodes TH, George AL, Jr (2008) Divergent biophysical defects caused by mutant sodium channels in dilated cardiomyopathy with arrhythmia. *Circ Res* 102(3):364–371.
29. Kochan LD, Churn SB, Omojokun O, Rice A, DeLorenzo RJ (2000) Status epilepticus results in an N-methyl-D-aspartate receptor-dependent inhibition of Ca^{2+}/calmodulin-dependent kinase II activity in the rat. *Neuroscience* 95(3):735–743.
30. Yamagata Y, Imoto K, Obata K (2006) A mechanism for the inactivation of Ca2+/calmodulin-dependent protein kinase II during prolonged seizure activity and its consequence after the recovery from seizure activity in rats in vivo. *Neuroscience* 140(3):981–992.
31. Liu XB, Murray KD (2012) Neuronal excitability and calcium/calmodulin-dependent protein kinase type II: Location, location, location. *Epilepsia* 53(Suppl 1):45–52.
32. Committee on Care and Use of Laboratory Animals (1996) *Guide for the Care and Use of Laboratory Animals* (Natl Inst Health, Bethesda), DHHS Publ No (NIH) 85–23.
33. Mistry AM, et al. (2014) Strain- and age-dependent hippocampal neuron sodium currents correlate with epilepsy severity in Dravet syndrome mice. *Neurobiol Dis* 65:1–11.
34. Lossin C, Wang DW, Rhodes TH, Vanoye CG, George AL, Jr (2002) Molecular basis of an inherited epilepsy. *Neuron* 34(6):877–884.
35. Rhodes TH, Lossin C, Vanoye CG, Wang DW, George AL, Jr (2004) Noninactivating voltage-gated sodium channels in severe myoclonic epilepsy of infancy. *Proc Natl Acad Sci USA* 101(30):11147–11152.
36. Kahlig KM, et al. (2008) Divergent sodium channel defects in familial hemiplegic migraine. *Proc Natl Acad Sci USA* 105(28):9799–9804.
37. Thompson CH, Kahlig KM, George AL, Jr (2011) *SCN1A* splice variants exhibit divergent sensitivity to commonly used antiepileptic drugs. *Epilepsia* 52(5):1000–1009.